

---

---

METALLURGY OF RARE  
AND NOBLE METALS

---

---

# Developmental Prospects of the Methods for Synthesizing Titanates of the Perovskite-Type Structure and Their Doping with Rare-Earth Elements

V. V. Cherepov<sup>a, \*</sup>, A. N. Kropachev<sup>a, \*\*</sup>, and O. N. Budin<sup>a, \*\*\*</sup>

<sup>a</sup>National University of Science and Technology “MISIS”, Moscow, 119049 Russia

\*e-mail: [tcherepovv@gmail.com](mailto:tcherepovv@gmail.com)

\*\*e-mail: [kan@misis.ru](mailto:kan@misis.ru)

\*\*\*e-mail: [o.n.budin@gmail.com](mailto:o.n.budin@gmail.com)

Received November 15, 2017; revised February 10, 2018; accepted February 19, 2018

**Abstract**—A review of methods for fabricating titanates of a perovskite-type structure and their doping with rare-earth elements is presented. The results of the scientific research of authors from different countries related to the study of the effect of doping titanates of the perovskite structure by rare-earth elements on their electromagnetic properties are discussed. The content of the work also includes information on the use of titanates of the perovskite-type structure in various industries. A comparative analysis of some morphological properties (particle size and structure) and electromagnetic characteristics (dielectric constant, Curie temperature, and modulus of longitudinal oscillations ( $d_{33}$ )) of powders fabricated (and doped) by different methods is carried out by the example of barium titanate ( $\text{BaTiO}_3$ ). Procedures for fabricating  $\text{BaTiO}_3$  by various methods, such as solvothermal, hydrothermal, sol–gel, chemical deposition, and solid-phase sintering, are described. The results of studying the influence of the variation in process parameters (temperature, pH, composition of the initial mixture of materials, and concentration of reagents) on the phase, morphology, and formation rate of  $\text{BaTiO}_3$  particles during the hydrothermal synthesis (with the use of  $\text{BaCl}_2$ ,  $\text{TiCl}_4$ , and  $\text{NaOH}$  as initial materials) are presented. The experiments on studying the influence of the microwave-radiation power during the solid-phase sintering of  $\text{BaCO}_3$  and  $\text{TiO}_2$  on dielectric and ferroelectric properties of  $\text{BaTiO}_3$  are also presented. An analysis of fabrication methods of  $\text{BaTiO}_3$  and its doping by rare-earth elements results in the statement that the hydrothermal method and solid-phase sintering, including the application of the microwave radiation, are currently the most promising fabrication technologies of materials with the perovskite-type structure with specified properties.

**Keywords:** titanates, perovskite, perovskite-type structure, synthesis, synthesis methods, doping, fine powders, nanomaterials, nanoparticles

**DOI:** 10.3103/S1067821219010024

## INTRODUCTION

Currently, the necessity of solving developmental problems and improving technologies related with the development of new alternative energy sources (systems) and energy carriers, as well as technologies associated with protecting humans from a complex of negative factors of the chemical, physical, and biological nature, is a primary task of scientists.

Solving such problems, in any event, implies the use of new constructional and composite materials, including ceramic and nanostructured ones, as well as multifunctional coatings possessing a series of unique properties. Such materials and coatings can have different crystalline natures. Materials with the perovskite and perovskite-type structure are of special interest.

The investigation into perovskites and materials with the perovskite-type structure is a very broad field of researches promising for scientific discoveries [1]. Perovskites are one of the broadest and most commonly met structural families in the solid-state chemistry. The perovskite structure makes it possible to include numerous cations and anions, as well as admit distortions and stoichiometry discrepancies; therefore, compounds belonging to this class have a wide spectrum of physicochemical properties [2], which determine their wide application in various fields (branches) of industry.

It is known from investigations that titanates with the perovskite-type structure possess high electromagnetic, catalytic, optical, and luminescent characteristics, as well as chemical resistance and thermal stability [3–5].

In this work, we fulfilled the review of the formation methods of finely dispersed powders of titanates with a perovskite-type structure and their doping with rare-earth elements.

The topicality of our work is in the collection of generalizing data on developments in this field in order to form investigatory procedures and fabricate titanates with a perovskite structure (in particular, europium titanate), as well as their doping with rare-earth elements and possessing optical and electromagnetic properties of interest, which determine their application in photovoltaics and radiospectroscopy.

#### APPLICATION REGIONS OF TITANATES WITH A PEROVSKITE-TYPE STRUCTURE

The uniqueness of electromagnetic properties of titanates with a perovskite-type structure is due to the fact that the compounds of this class are multiferroics; i.e., two or more “ferro”-ordering types coexist simultaneously in them, notably, ferromagnetic, ferroelectric, and ferroelastic. Ferromagnetics (or magneto-electrics) are a particular case of multiferroics.

Magnetolectric materials can find wide application in sensor technology, microwave devices, and spintronics, as well as in memory devices (magneto-electric domains can be used as bits) [6].

The most striking representatives of this class of materials, which have already found practical application in electronics, are titanates of barium  $\text{BaTiO}_3$ , strontium  $\text{SrTiO}_3$ , and calcium  $\text{CaTiO}_3$ . Titanates  $\text{CaTiO}_3$  and  $\text{BaTiO}_3$  are used as insulators in multilayered ceramic capacitors [7]. In addition,  $\text{BaTiO}_3$  is used as the material for piezoceramic emitters and piezoelectric microphones, it also serves the bases for solid solutions in the production of thermoresistors (thermistors) with a positive temperature-resistance coefficient. The use of  $\text{BaTiO}_3$  in thermoelectric energy converters also considered promising [8].

The introduction of doping impurities (La, Sb, Zn, Sn, Ce, Zr, and Hf) into barium titanate extends its application and enables its use in electromechanical and electrooptical systems as pyroelectric detectors and piezoelectric drives, as well as in microelectromechanical systems and devices with ferroelectric operative memory (FeRams), etc. [9].

Strontium titanate  $\text{SrTiO}_3$  is used as a component in the fabrication of ferroelectric ceramics and as a nonlinear dielectric material. Single crystals of  $\text{SrTiO}_3$  are widely used as substrates for growing thin films of high-temperature superconductors and ferroelectrics. In addition, it is noted that the use of  $\text{SrTiO}_3$  is highly promising in thin-film capacitors [10].

The authors of [11] established that the doping of  $\text{SrTiO}_3$  by donor rare-earth elements (REs) according to the composition  $\text{Sr}_{1-x}\text{RE}_x\text{TiO}_3$  can transform its conduction from insulator to semiconductor, espe-

cially at high temperatures. Investigations resulted in studying the RE-doping of strontium titanate, including doping with  $\text{Gd}^{3+}$  ions, to fabricate n-type semiconductor materials for energy “harvesting” from any external sources (energy harvesting applications).

Investigations [12] showed that the permittivity of ceramics with the  $\text{Sr}_{1-1.5x}\text{Dy}_x\text{TiO}_3$  composition, especially with  $x = 0.01$ , are higher than for undoped  $\text{SrTiO}_3$  at both low and room temperatures. The ceramic material with the  $\text{Sr}_{0.985}\text{Dy}_{0.01}\text{TiO}_3$  composition possesses high permittivity of  $\sim 33\,500$  at 28 K and  $\sim 9600$  at room temperature with a moderate dissipation coefficient of  $\sim 0.02$ . This fact makes the ceramic more promising for application in capacitors when compared with  $\text{SrTiO}_3$ .

At the same time, the permittivity of  $\text{Sr}_{0.985}\text{Dy}_{0.01}\text{TiO}_3$  ceramics is close to the permittivity of  $\text{Sr}_{0.985}\text{Y}_{0.01}\text{TiO}_3$  ceramics, which is conditioned by the similarity of ion radii of yttrium and dysprosium [12]. A similar regularity was noted stoichiometric (undoped) titanates with a perovskite structure. Both  $\text{SrTiO}_3$  and  $\text{EuTiO}_3$  have identical unit-cell parameters and are able to nucleate ferroelectric instabilities at low temperatures [3, 13]. This fact can be the basis for new studies in this subject region.

The application of  $\text{CaTiO}_3$  is promising in biomedicine (composite coatings for titanium-based prosthetic alloys) [14, 15], solar photovoltaics (solar cells) [16], electronics for the fabrication of highly sensitive thermoresistors (thermistors) with a negative temperature-resistance coefficient [17], and radiation safety (the use of ceramics based on calcium aluminotitanate with the perovskite structure for hardening and disposal of radionuclides) [18]. Ceramic titanate  $\text{CaTiO}_3$  is also a good candidate for application in electron microwave devices due to its high cavity quality coefficient ( $Q_u = 8000$  at 1.5 GHz) [4], where  $Q_u = Q/f$ , where  $Q$  is the figure of merit and  $f$  is the frequency.

We should note alloys of  $\text{CaTiO}_3$  with magnesium titanate  $\text{MgTiO}_3$  ( $Q_u = 8000$  at 7.75 GHz) and magnesium strontium niobate  $\text{Sr}(\text{Mg}_{1/3}\text{Nb}_{2/3})\text{O}_3$  ( $Q_u = 20000$  at 1.5 GHz), which possess outstanding dielectric properties, enabling their application in dielectric devices of cavities, filters, and antennas operating in a microwave range [4].

According to investigations [4], the luminescence data showed that  $\text{Ca}_{1-x}\text{Mg}_x\text{TiO}_3$  and  $\text{Ca}_{1-x}\text{Mg}_{x/2}\text{Eu}_{2y/3}\text{TiO}_3$  powders could be used as materials for the fabrication of lighting units based on UV radiation and blue LED using an excitation wavelength of 397 and/or 450 nm.

It is proven that the doping of titanates with a perovskite-type structure by rare-earth elements and such charge compensators as  $\text{Al}^{3+}$ ,  $\text{In}^{3+}$ ,  $\text{Ga}^{3+}$ ,  $\text{Mg}^{2+}$ ,  $\text{Zn}^{2+}$ , and  $\text{Li}^+$  improve luminescent properties. For example,  $\text{Li}^+$  ions in  $\text{CaTiO}_3$  perovskite doped with thin  $\text{Pr}^{3+}$

and  $\text{Li}^+$  films,  $\text{Li}^+$  ions increase the quantum efficiency of radiation, as well as promote both certain morphological changes and variations in grain sizes of particles [4].

For example, as far back as in 2007, the authors of [19] affirmed that the doping of titanates with a perovskite structure ( $\text{Pb}(\text{Zr},\text{Ti})\text{O}_3$ ,  $\text{BaTiO}_3$ , and  $\text{PbTiO}_3$ ) by ions of rare-earth elements with optical activity such as  $\text{Eu}^{3+}$ ,  $\text{Er}^{3+}$ ,  $\text{Pr}^{3+}$ ,  $\text{Sm}^{3+}$ , and  $\text{Nd}^{3+}$  can lead to new investigations into the luminescent properties of this class of materials, which will be very a interesting attribute for modern technologies.

Currently, the attention of many scientists is focused on the fabrication and investigation of titanates with the perovskite-type structure, including doped with rare-earth elements.

#### FABRICATION AND DOPING METHODS OF TITANATES WITH THE PEROVSKITE-TYPE STRUCTURE

Properties of compounds with the perovskite-type structure depend strongly on the fabrication method. For example, the use of the coprecipitation method can lead to a well-crystallized structure, while the nanocasting method (complementary synthesis) makes it possible to attain perovskites with a large surface area. Therefore, depending on the final use, the desired properties of this class of materials can be attained by selecting the proper synthesis method [20, 21].

Titanates with a perovskite-type structure can be synthesized by different methods. For example, according to [3], high-quality nanoparticles of europium titanate  $\text{EuTiO}_3$  were fabricated using the sol-gel method. In addition, the authors of [4] describe the fabrication of  $\text{CaTiO}_3$  powders doped with magnesium and europium ions, which is based on the method of polymer precursors. In addition to the abovementioned methods, solid-phase synthesis [22, 23], hydrothermal synthesis (including with the use of microwave radiation) [24, 25], chemical precipitation (coprecipitation) methods, and mechanochemical synthesis are very popular for the formation of titanates and complex oxides.

It was already noted that  $\text{BaTiO}_3$  is one well-studied titanate with a perovskite structure. Therefore, the reflection of the dependence of properties (morphological and electromagnetic) of titanate powders with the perovskite structure on their fabrication method (as well as their doping methods) will be especially demonstrative using the example of  $\text{BaTiO}_3$ .

#### *Comparison of Properties of $\text{BaTiO}_3$ Samples Doped with Europium Ions when Using Various Methods*

To compare characteristics of  $\text{BaTiO}_3$  powders doped with europium ions, we selected the hydrother-

mal method described in [26] and solid-phase sintering method (studies [27]).

The hydrothermal method included the preparation of the mixture of  $\text{Ba}(\text{OH})_2 \cdot 8\text{H}_2\text{O}$  and  $\text{TiO}_2$  at molar ratio  $\text{Ba}/\text{Ti} = 1.64$ . Subsequently, the specified amount of europium hydrate acetate was added to a mixture. Then the content was placed into an autoclave and held for 3 h at  $150^\circ\text{C}$ . After the reaction was completed, the content was cooled to  $80^\circ\text{C}$  and formic acid was added to remove undesirable carbonates. Then the products were filtered, rinsed with hot distilled water, and dried in a furnace at  $100^\circ\text{C}$  for 12 h. In such a manner, five Eu-doped samples with the ratio of mol %  $\text{Eu}/\text{Ti}$  of 0.05, 0.1, 0.15, 0.2, and 0.25 were synthesized. The samples were annealed at  $1000^\circ\text{C}$  for 2 h in a muffle furnace. Granules were compacted for further studies ( $15 \text{ t}/\text{cm}^2$ ) and repeatedly annealed at 200, 500, 700, and  $1000^\circ\text{C}$  for 2 h each.

Polycrystalline samples with the  $\text{BaTiO}_3 + \text{X}$  composition (where X is the content of  $\text{Eu}_2\text{O}_3 = 1, 2, \text{ and } 3 \text{ wt } \%$ ) were fabricated by solid-phase sintering.

When comparing different doping methods, it was established that more finely dispersed particles (20–45 nm) are formed when using the hydrothermal method when compared with the solid-phase sintering (1.5–2.5  $\mu\text{m}$ ). Herewith, the hydrothermal method makes it possible to form particles with the cubic structure (only subsequent annealing promotes the formation of the tetragonal structure), while solid-phase sintering makes it possible to form the tetragonal structure.

In addition, a variation in electromagnetic properties was noted in both cases with respect to stoichiometric  $\text{BaTiO}_3$ . Maximal permittivity for all samples synthesized by solid-phase sintering was fixed at approximately the same temperature of  $\sim 400 \text{ K}$  (the Curie temperature) (Fig. 1) [27].

The maximal permittivity at this temperature was determined for the sample containing no europium ions. Herewith, it was noted that permittivity decreased with an increase in the europium content in the samples (the dependence is linear). An inverse phenomenon was observed at room temperature, and the sample with the highest content of europium ions had maximal permittivity.

At the same time, no dependence of the dielectric constant (DC) on the  $\text{Eu}/\text{Ti}$  ratio (Fig. 2) can be followed for the samples formed by the hydrothermal synthesis [26].

The Curie temperatures of the samples are in a range from 80 to 120 K (at 1 kHz). The maximal dielectric constant (10 576) is fixed for the sample with ratio  $\text{Eu}/\text{Ti} = 0.15$ . The dielectric constant for the sample with ratio  $\text{Eu}/\text{Ti} = 0.2$  is larger than for the samples with the  $\text{Eu}/\text{Ti}$  ratio of 0.05 and 0.1 (which in turn have almost identical values). Herewith, the dielectric constant of stoichiometric  $\text{BaTiO}_3$  overall

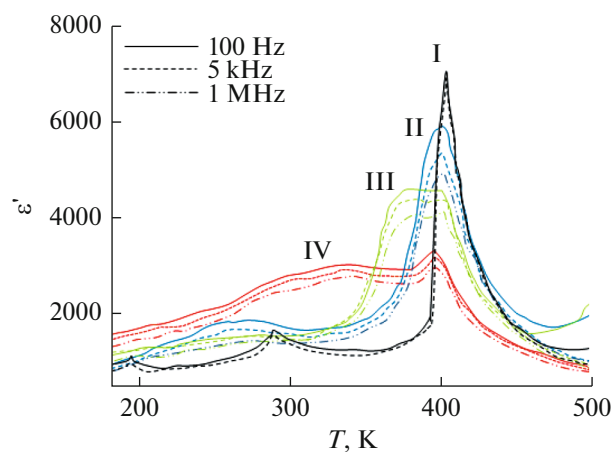


**Fig. 1.** Temperature dependence of permittivity (adopted from [27]). Here, curves I, II, III, and IV correspond to the samples with the composition  $\text{BaTiO}_3 + X \text{ wt } \% \text{Eu}_2\text{O}_3$  at  $X = 0, 1, 2,$  and  $3,$  respectively.

the temperature range is minimal with respect to presented samples.

Thus, the comparison showed that some electromagnetic characteristics (in particular, the Curie temperature and permittivity) for materials doped by different methods are substantially different.

#### *Comparison of Morphological Properties of $\text{BaTiO}_3$ Samples Formed by Various Methods*

According to [28], when using the solvothermal method, in which the  $\text{BaTi}(\text{OR})_6$  precursor was formed by mixing  $\text{Ba}(\text{OR})_2$  and  $\text{Ti}(\text{OR})_4$  in benzene, we synthesized the particles with an average size smaller than 20 nm ((OR) means alkoxide). Solutions were formed by the dissolution of metallic barium and titanium isopropoxide  $\text{Ti}(\text{OC}_3\text{H}_7)_4$  in a mixture of anhydrous benzene and isopropanol, which was accompanied by the formation of the  $\text{BaTi}[\text{OC}_3\text{H}_7]_6$  precursor. Herewith, the coexistence of tetragonal and cubic phases was revealed for the particles.

Barium titanate powders fabricated by a hydrothermal method in a temperature range of 100–200°C during the interaction of fine  $\text{TiO}_2$  particles with a strongly alkaline solution ( $\text{pH} > 12$ ) of  $\text{Ba}(\text{OH})_2 \cdot \text{TiCl}_4$  had a particle size in a range from 50 to 400 nm [28]. This method implies the two-stage deposition mechanism. The first synthesis stage includes the formation of the Ti-rich amorphous precipitate. The second synthesis stage is the reaction between the amorphous phase and  $\text{Ba}^{2+}$  ions that remained in the solution, which leads to the crystallization of  $\text{BaTiO}_3$ . A similar method is described in [29], but  $\text{BaCl}_2$ ,  $\text{TiCl}_4$ , and  $\text{NaOH}$  were used as the initial materials. The influence of the variation in working parameters such as the temperature, pH, the composition of the initial mate-

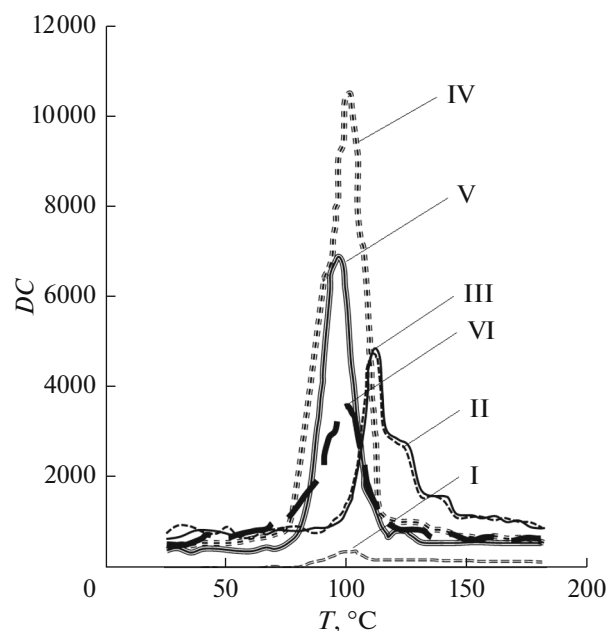


**Fig. 2.** Influence of doping  $\text{BaTiO}_3$  with europium ions on the dielectric constant and Curie temperature (adopted from [26]). Here, I is stoichiometric  $\text{BaTiO}_3$ ; II, III, IV, V, and VI are the samples with the  $\text{Eu}/\text{Ti}$  ratio of 0.05, 0.1, 0.15, 0.2, and 0.25, respectively.

rial mixture, and reagent concentration on the phase, morphology, and formation rate of  $\text{BaTiO}_3$  particles was investigated. The investigation into the influence of each parameter was performed at constant other parameters (the results of investigations are shown in Table 1).

It is seen from Table 1 that the reaction temperature pronouncedly affects the final products (samples nos. 1–5). No formation of  $\text{BaTiO}_3$  particles was observed at room temperature even after a very prolonged time (12 h) because of the slow kinetics. Pseudocubic  $\text{BaTiO}_3$  was found at 60°C and above with a small amount of the secondary phase consisting of  $\text{BaCO}_3$ . An increase in temperature leads to improving the  $\text{BaTiO}_3$  crystallinity, and an increase in the reaction rate makes it possible to avoid the excessive contamination with  $\text{CO}_2$  and, correspondingly, the subsequent formation of the  $\text{BaCO}_3$  impurity.

When studying the influence of the composition of the initial mixture of materials (samples no. 5–9), it was established that amorphous, irregular, and aggregated compounds with numerous particles are formed at molar ratio  $[\text{BaCl}_2]/[\text{TiCl}_4] < 1.0$ , but spherical particles of pseudocubic  $\text{BaTiO}_3$  are formed at  $[\text{BaCl}_2]/[\text{TiCl}_4] > 1.0$ . The particle size insignificantly decreased with the further increase in molar ratio  $[\text{BaCl}_2]/[\text{TiCl}_4]$ .

We also determined the critical threshold of the  $\text{BaCl}_2$  concentration of about 0.1 mol/L (samples

**Table 1.** Experimental parameters and preparation characteristics of BaTiO<sub>3</sub> (adopted from [29])

No.	<i>T</i> , °C	[NaOH], mol/L	[BaCl <sub>2</sub> ], mol/L	[BaCl <sub>2</sub> ]/[TiCl <sub>4</sub> ]	Primary phase	Secondary phase	Morphology	Particle size, nm
1	25	6.0	0.5	1.07	AM	BC, NA	I, A	
2	60	6.0	0.5	1.07	BT	BC, AM	S, A	110
3	75	6.0	0.5	1.07	BT	BC	S, A	90
4	80	4.0	0.5	1.07	BT	BC	S	80
5	90	6.0	0.5	1.07	BT		S	60
6	90	6.0	0.5	0.8	AM	BT	I, A	
7	90	6.0	0.5	0.95	BT	AM	S, I, A	80
8	90	6.0	0.5	1.15	BT		S	60
9	90	6.0	0.5	1.2	BT	BC	S	60
10	90	6.0	0.1	1.07	AM, BC	BT	I, A, S	
11	90	6.0	0.05	1.07	AM, BC		I, A	
12	90	6.0	0.2	1.07	BT	BC	I, S	90
13	90	6.0	0.7	1.07	BT		S	50
14	90	6.0	1.0	1.07	BT		S	40
15	90	2.0	0.5	1.07	AM	BC, NA	A, I	
16	90	3.5	0.5	1.07	BT	AM, BC	S, A	100

AM: amorphous phase; BC: BaCO<sub>3</sub>; BT cubic BaTiO<sub>3</sub>; and NA: NaCl. S: spherical; A: aggregates; I: irregular shape.

nos. 5, 10–14). Above this value, the total BaTiO<sub>3</sub> conversion can be attained for several minutes and, below this value, the crystallization occurred considerably more slowly (herewith, the precipitate had Ba/Ti < 1). This is explained by the fact that the higher reagent concentrations lead to higher nucleation rates forming the larger number of small nuclei, which promotes the precipitation of particles with a considerably smaller size and uniform size distribution. However, the excessively high concentration can affect the separation of Ba(OH)<sub>2</sub> · 8H<sub>2</sub>O from the solution, which can affect the precise control of the Ba/Ti molar ratio.

It is established that the precipitation reaction with a high OH<sup>-</sup> concentration holds a high degree of supersaturation in the reaction systems, which improves the crystallinity of BaTiO<sub>3</sub>. A pure and clearly pronounced cubic BaTiO<sub>3</sub> phase was formed at high pH ( $C_{\text{NaOH}} \geq 6.0$  mol/L), while the particles formed at low pH ( $C_{\text{NaOH}} \leq 2.0$  mol/L) were irregular and aggregated (samples no. 5, 16, and 16).

The authors of [30] considered two variants of formation of BaTiO<sub>3</sub> according to the sol–gel method. In the first variant, tetrabutyl titanate (0.1 mol) was dissolved in isopropanol at room temperature and then anhydrous acetic acid (0.3 mol) was added with stirring for 0.5 h and formation of titanyl acetate. Then the precipitation was performed by the introduction of titanyl acetate into the aqueous solution of acetic acid containing barium acetate (0.1 mol). The value of pH was brought to 3.0–4.0 by adding anhydrous acetic acid. A mixture was stirred for 0.5 h until a transparent

sol was formed. Then, holding at 95°C until gel was formed and drying in a furnace at 120°C for 12 h were performed. Finally, to form BaTiO<sub>3</sub> nanopowders, dried gel was calcined in air at various temperatures.

In the second variant, a fixed amount of barium stearate was added to molten stearic acid, forming a transparent yellow solution. Then a stoichiometric amount of tetrabutyl titanate was introduced into the solution under stirring, which resulted in the formation of homogeneous brown sol. Then natural cooling to room temperature and drying for 12 h for the gel formation followed. Then the gel was calcined at various temperatures in air to form BaTiO<sub>3</sub> nanocrystallites.

The average size of the particles of synthesized powders was 50–80 nm for the first and 25–50 nm for the second case.

The authors of [31] described the method of BaTiO<sub>3</sub> formation (the precipitation by oxalic acid). The barium-containing solution was formed by mixing barium acetate, deionized water, and alcohol. Then the titanium-containing solution was formed by the dissolution of tetra-*n*-butyl titanate in the solution of alcohol and oxalic acid. Then solutions were mixed together under continuous stirring. Then drying and calcination processes followed. This resulted in the formation of BaTiO<sub>3</sub> particles, the size of which was 38.2 nm. It was also revealed that the formation of pure BaTiO<sub>3</sub> occurs at a calcination temperature no lower than 800°C. Herewith, the transition of the crystalline structure from the cubic crystal system into the

**Table 2.** Comparison of synthesis and doping methods of BaTiO<sub>3</sub>

Synthesis method	Particle size, nm	Morphology (structure)	Reference
Synthesis			
Solvothermal	<20	Coexistence of cubic and tetragonal	[28]
Hydrothermal	50–400	Cubic; amorphous	[29]
Sol–gel	25–80	No data	[30]
Chemical	40	Cubic; tetragonal (after calcination)	[31]
Doping			
Hydrothermal	20–45	Cubic; tetragonal (after annealing)	[26]
Solid-phase sintering	1600–2500	Tetragonal	[27]

tetragonal one was fixed at a calcination temperature higher than 1000°C.

Thus, using various synthesis methods and varying the process parameters, we can form materials with various particle morphologies. The comparison of synthesis methods (and doping with europium ions) of BaTiO<sub>3</sub> by the coarseness of formed particles is presented in Table 2.

#### *Influence of Microwave Radiation Power on Properties of BaTiO<sub>3</sub> Ceramics during Solid-Phase Sintering*

Results of investigations into the influence of microwave radiation power on dielectric and ferroelectric properties of BaTiO<sub>3</sub> ceramics formed by solid-phase sintering with initial materials BaCO<sub>3</sub> and TiO<sub>2</sub> are presented in [32]. The authors used MRF16/22-CMAT (Carbolite Microwave Assist Technology) hybrid furnace with a microwave power of 1.8 kW operating at a frequency of 2.45 GHz, in addition to heaters made of molybdenum silicide (9 kW). Investigations were performed at the microwave radiation power of 0, 15, 30, 50, and 75%.

The variation in permittivity ( $\epsilon$ ) and surface-charge density of the samples ( $Q_{sw}$ ), as well as the particle-size distribution of the samples formed during sintering at various values of microwave radiation power, are

presented in Figs. 3, 4, and 5, respectively ( $\epsilon$  was measured at room temperature).

It is seen from Figs. 3 and 4 that the maximal permittivity and surface charge density are observed for the sample formed during sintering with the use of 30% power of microwave radiation. According to the data presented in the article, permittivity increased by 58%, while the surface charge density increased by 17% with respect to the sample, which was formed without microwave radiation.

The observed enhancement in dielectric and ferroelectric properties of the sample can be explained from the viewpoint of the microstructure and grain-size uniformity. The influence of the particle size on electromagnetic properties of BaTiO<sub>3</sub> ceramics are rather widely described in scientific publications. The enhancement of electromagnetic and ferroelectric properties is characteristic of the grain size in a range of 1.7–0.5  $\mu\text{m}$ , considerably worsening for grains smaller than 0.5  $\mu\text{m}$  and vanishing for coarseness of 10–30 nm [32].

Thus, these results evidence the possibility of controlling functional properties of BaTiO<sub>3</sub> ceramics by using the microwave radiation.

#### *Comparison of Certain Electromagnetic Properties of Particles and BaTiO<sub>3</sub> Ceramics Formed by Various Methods*

The authors of [28] established that, when fabricating barium titanate particles in the form of compact systems (granules formed by solid-phase sintering),

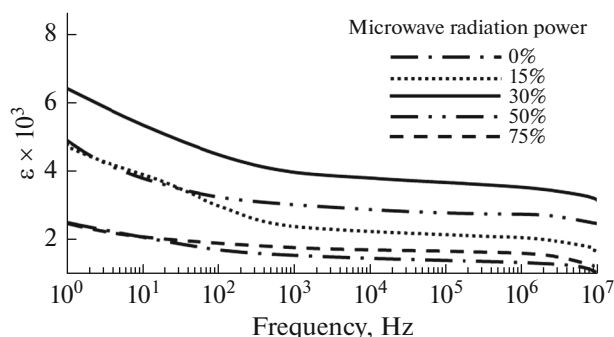


**Fig. 3.** Variation in permittivity ( $\epsilon$ ) at room temperature (Adopted from [32]).

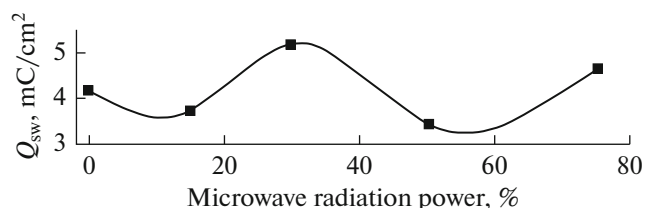


**Fig. 4.** Variation in surface charge density of samples ( $Q_{sw}$ ) (adopted from [32]).

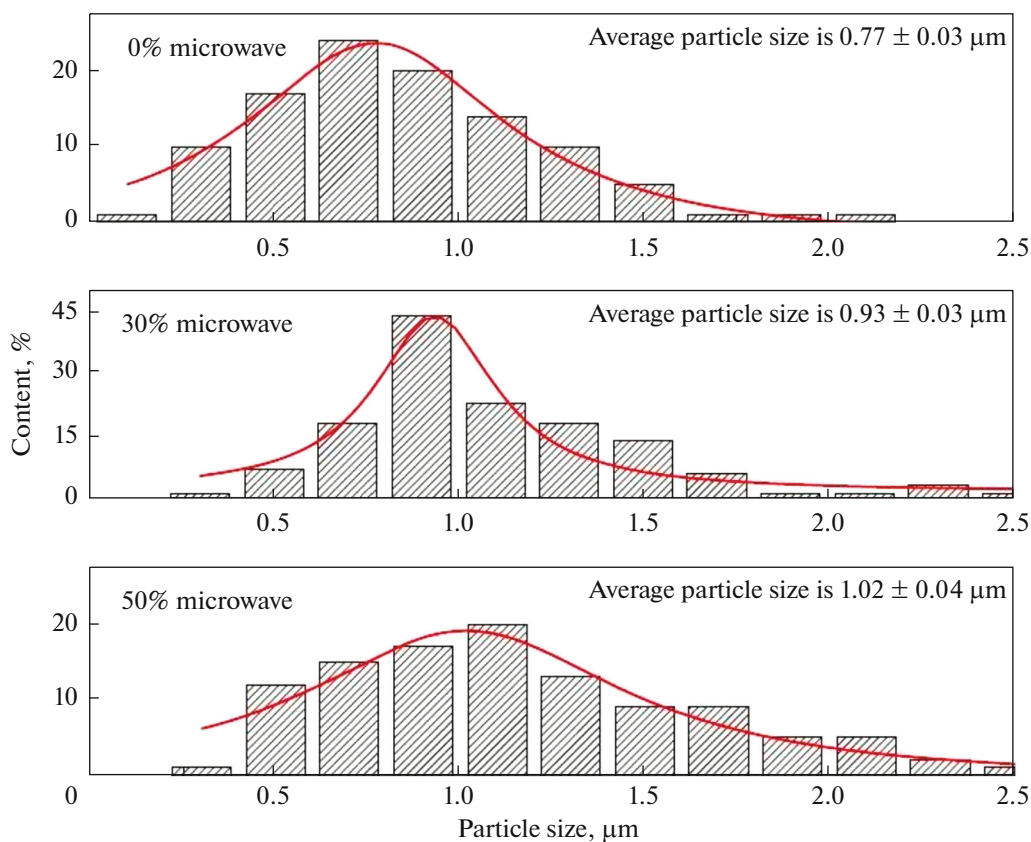


Fig. 5. Particle-size distribution (adopted from [32]).

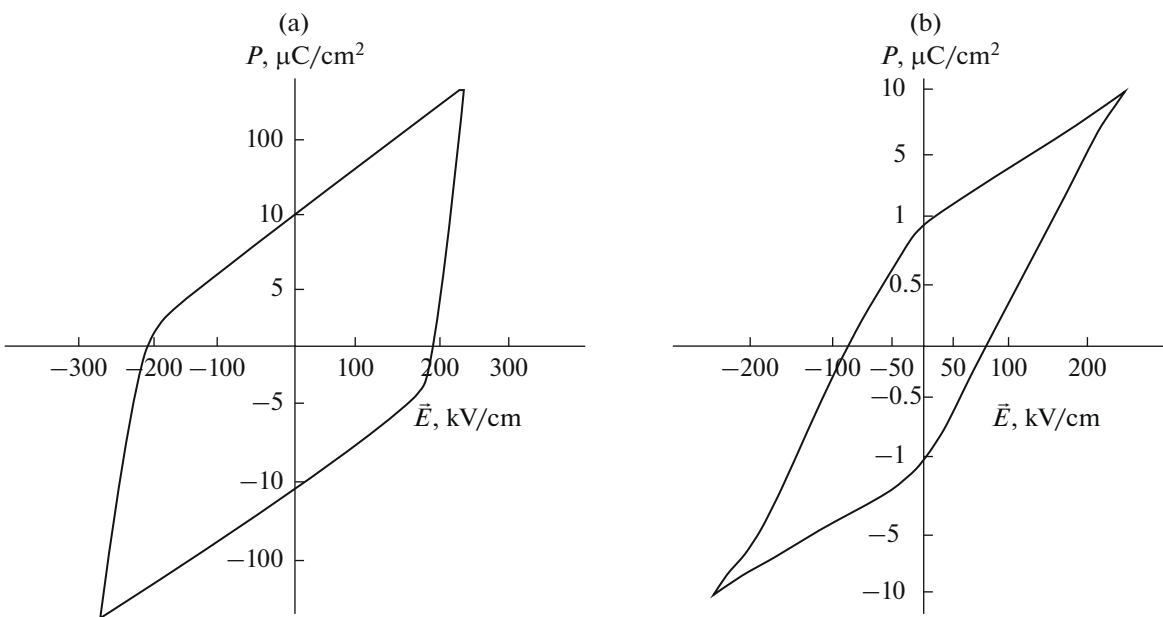


Fig. 6. Dependence of polarization on the electric field strength for (a) compact systems and (b) dispersed particles of barium titanate (adopted from [28]).

the hysteresis loop (the dependence of polarization on the electric field strength) turns out wide and extended (Fig. 6a). Such a form is inherent to hard-magnetic materials having a high coercive force and residual

magnetic induction. At the same time, when forming dispersed particles (in the case of using the polymer precursor method), the plot of the polarization dependence on the electric field strength turns out narrow

with long ends, which is characteristic of soft-magnetic materials (Fig. 6b). Herewith, the residual polarization in the case of compact nanoparticles ( $10 \mu\text{C}/\text{cm}^2$ ) is tenfold higher when compared with dispersed nanoparticles ( $1 \mu\text{C}/\text{cm}^2$ ).

A comparison of piezoelectric properties of  $\text{BaTiO}_3$  ceramics formed by solid-phase sintering (sintering of  $\text{BaCO}_3$  and  $\text{TiO}_2$  powders) and oxalic precipitation showed a substantial difference in piezoelectric modulus  $d_{33}$  (modulus of longitudinal oscillations), 419 and 260 pC/N, respectively [28].

Based on the above, we can conclude that currently there are several basic methods of the synthesis and doping of titanates with the perovskite structure (further perovskites). Materials are widely presented in scientific publications, in which the results of investigations into electromagnetic, optical, and morphological properties of perovskites prepared and doped by one or another method are reflected. However, the formation of perovskites with specified properties causes significant difficulties. Therefore, the revelation of efficient synthesis methods of perovskites with specified properties is of large scientific interest. The generalization of the results of scientific publications showed that the hydrothermal method is most examined in this field. The solid-phase sintering method can be considered the most promising, including that with the application of the microwave radiation.

## CONCLUSIONS

In this article, we considered the methods of formation of titanates with the perovskite-type structure and their doping methods by rare-earth elements (using the example of barium titanate).

Currently, numerous methods of the synthesis and doping of titanates with the perovskite structure are known, each of which has definite peculiarities.

The methods of formation of titanates and doped titanates with the perovskite-type structure from solutions (in particular, the hydrothermal method), when compared with solid-phase methods, make it possible to fabricate purer and more finely dispersed nanopowders and it is simpler to control the particle morphology of the fabricated material with their help. At the same time, the solid-phase sintering method makes it possible to form particles in the form of compact systems, the character of electromagnetic properties of which substantially differs from materials fabricated from solutions.

Thus, when varying the fabrication methods of titanates and their doping methods with REEs, we can fabricate materials with the perovskite-type structure with specified radiospectrometric properties (for example, absorption and reemission) similar in composition but completely different in structure and magnetoelectric characteristics. They find application in rapidly developing promising industries as solar-

power engineering, optoelectronics, thermoelectrics, and the military–industrial complex.

According to our analysis, the most promising current method of fabricating materials with the perovskite-type structure with the specified properties is the solid-phase sintering (including the application of the microwave radiation).

## REFERENCES

1. Dogan, Fatih, Lin, Hong, Guilloux-Viry, Maryline, and Peña, Octavio, Focus on properties and applications of perovskites, *Sci. Technol. Adv. Mater.*, 2015, vol. 16, no. 2. doi 10.1088/1468-6996/16/2/020301.
2. Artini, C., Crystal chemistry, stability and properties of interlanthanide perovskites: A review, *J. Eur. Ceram. Soc.*, 2016, vol. 37, no. 2, pp. 427–440. <https://doi.org/10.1016/j.jeurceramsoc.2016.08.041>.
3. Wei, T., Liu, H.P., Chen, Y.F., Yan, H.Y., and Liu, J.-M., Preparation, magnetic characterization, and optical band gap of  $\text{EuTiO}_3$  nanoparticles, *Appl. Surf. Sci.*, 2011, vol. 257, no. 2, pp. 4505–4509. <https://doi.org/10.1016/j.apsusc.2010.12.112>.
4. Oliveira, Larissa H., Savioli, de Moura, Julia Ana P., Nogueira, Icamira C., Li, Maximo S., Longo, Elson, Varela, Jose A., and Rosa, Ieda L.V., Investigation of structural and optical properties of  $\text{CaTiO}_3$  powders doped with  $\text{Mg}^{2+}$  and  $\text{Eu}^{3+}$  ions, *J. Alloys Compd.*, 2015, vol. 647, pp. 265–275. <https://doi.org/10.1016/j.jallcom.2015.05.226>.
5. Sankovich, A.M., The mechanism of formation, thermal stability, and thermodynamic properties of cationically ordered perovskite-like layered oxides  $\text{ALnTiO}_4$  and  $\text{A}_2\text{Ln}_2\text{Ti}_3\text{O}_{10}$  ( $\text{A} = \text{Na}, \text{K}, \text{Ln} = \text{Nd}, \text{Gd}$ ), *Extended Abstract of Cand. Sci. Dissertation*, St. Petersburg: St. Petersburg Gos. Univ., 2012.
6. Kravtseva, M.S., Synthesis and properties of thin epitaxial  $\text{BiFeO}_3$  films and solid solutions based on it, *Extended Abstract of Cand. Sci. Dissertation*, Moscow: Mos. Gos. Univ., 2008.
7. New MLCC technology for the production of large-size ceramic capacitors. [http://kit-e.ru/assets/files/pdf/2009\\_06\\_12.pdf](http://kit-e.ru/assets/files/pdf/2009_06_12.pdf) (accessed June 20, 2017).
8. Gridnev, S.A., Electrical properties of semiconductor ceramics based on barium titanate, *Vestn. Voronezh. Gos. Tekh. Univ.*, 2012, vol. 8, no. 11, pp. 57–61.
9. Vijatovic Petrovic, M.M., Grigalaitis, R., Ilic, N., Bobic, J.D., Dzunuzovic, A., Banys, J., and Stojanovic, B.D., Interdependence between structure and electrical characteristics in Sm-doped barium titanate, *J. Alloys Compd.*, 2017, vol. 724, pp. 959–968. <http://dx.doi.org/10.1016/j.jallcom.2017.07.099>.
10. Anaraki, S., Thin-film capacitor based on strontium titanate formed by the sol–gel method, *Mikroelektronika*, 2015, vol. 44, no. 6, pp. 476–480.
11. Tkach, Alexander, Amaral, Joao S., Amaral, Vitor S., and Vilarinho, Paula M., Dielectric spectroscopy and magnetometry investigation of Gd-doped strontium titanate ceramics. *J. Eur. Ceram. Soc.*, 2017, vol. 37, no. 6, June, pp. 2391–2397. <https://doi.org/10.1016/j.jeurceramsoc.2017.02.011>.



12. Tkach, Alexander, Amaral, Joao S., Zlotnik, Sebastian, Amaral, Vitor S., and Vilarinho, Paula M., Enhancement of the dielectric permittivity and magnetic properties of Dy substituted strontium titanate ceramics, *J. Alloys Compd.*, <https://doi.org/10.1016/j.jeurceramsoc.2017.09.007>.
13. Electrical Properties of Un-Doped and Doped  $\text{EuTiO}_3$ -Based Perovskites. [http://theses.whiterose.ac.uk/4064/1/University\\_of\\_Sheffield\\_-final\\_thesis-1.pdf](http://theses.whiterose.ac.uk/4064/1/University_of_Sheffield_-final_thesis-1.pdf) (accessed June 24, 2017).
14. Daqing Wei, Yu Zhou, Dechang Jia, and Yaming Wang, Formation of  $\text{CaTiO}_3/\text{TiO}_2$  composite coating on titanium alloy for biomedical applications, *J. Biomed. Mater. Res.*, 2008, vol. 84B, no. 2, pp. 444–451. doi 10.1002/jbm.b.30890
15. Manso, Miguel, Langlet, Michel, and Martinez-Duart, J.M., Testing sol–gel  $\text{CaTiO}_3$  coatings for bio-compatible applications, *Mater. Sci. Eng.*, 2003, vol. 23, no. 3, pp. 447–450, [https://doi.org/10.1016/S0928-4931\(02\)00319-3](https://doi.org/10.1016/S0928-4931(02)00319-3).
16. Better than silicon. <http://spkurdyumov.ru/uploads//2015/08/luchshe-kremniya.pdf> (accessed June 23, 2017).
17. Sahoo, Subhanarayan, Parashar, S.K.S., and Ali, S.M.,  $\text{CaTiO}_3$  nano ceramic for NTCR thermistor based sensor application, *J. Adv. Ceram.*, 2014, vol. 3, no. 2, pp. 117–124. doi 10.1007/s40145-014-0100-6
18. Bekman, I.N. et al, Emanation-thermal analysis of perovskite, *Radiokhimiya*, 2004, vol. 46, no. 3, pp. 272–279.
19. Paris, E.C., Espinosa, J.W.M., de Lazaro, S., Lima, R.C., Joya, M.R., Pizani, P.S., Leite, E.R., Souza, A.G., Varela, J.A., and Longo, E.,  $\text{Er}^{3+}$  as marker for order–disorder determination in the  $\text{PbTiO}_3$  system, *Chem. Phys.*, 2017, vol. 335, pp. 7–14. doi 10.1016/j.chemphys.2007.03.019
20. Zhu, J. and Thomas, A., Perovskite-type mixed oxides as catalytic material for NO removal. *Appl. Catal. B: Environ.*, 2009, vol. 92, nos. 3–4, pp. 225–233. <https://doi.org/10.1016/j.apcatb.2009.08.008>.
21. Zhu, J. and Chen, J., Perovskite-Type Oxides: Synthesis and Application in Catalysis. [https://www.novapublishers.com/catalog/product\\_info.php?products\\_id=23377](https://www.novapublishers.com/catalog/product_info.php?products_id=23377) (accessed June 25, 2017).
22. Yanhua Zong, Kazuma Kugimiya, Koji Fujita, Hirofumi Akamatsu, Kazuyuki Hirao, and Katsuhisa Tanaka, Preparation and magnetic properties of amorphous  $\text{EuTiO}_3$  thin films, *J. Non-Cryst. Solids*, 2010, vol. 356, pp. 2389–2392. <https://doi.org/10.1016/j.jnoncrsol.2010.05.014>.
23. Fengfeng Chi, Yanguang Qin, Shaoshuai Zhou, Xiantao Wei, Yonghu Chen, Changkui Duan, and Min Yin,  $\text{Eu}^{3+}$ -site occupation in  $\text{CaTiO}_3$  perovskite material at low temperature, *Current Appl. Phys.*, 2017, vol. 17, no. 1, pp. 24–30. <https://doi.org/10.1016/j.cap.2016.10.018>
24. Tatiana Martelli Mazzo, Ivo Mateus Pinatti, Leilane Roberta Macario, Waldir Avansi Junior, Mario Lucio Moreira, Ieda Lucia Viana Rosa, Valmor Roberto Mastelaro, Jose Arana Varela, and Elson Longo, Europium-doped calcium titanate: Optical and structural evaluations, *J. Alloys Compd.*, 2014, vol. 585, pp. 154–162. <https://doi.org/10.1016/j.jallcom.2013.08.174>.
25. Moreira, Mario L., Paris, Elaine C., do Nascimento, Gabriela S., Longo, Valeria M., Sambrano, Julio R., Mastelaro, Valmor R., Bernardi, Maria I.B., Andres, Juan, Varela, Jose A., and Longo, Elson, Structural and optical properties of  $\text{CaTiO}_3$  perovskite-based materials obtained by microwave-assisted hydrothermal synthesis: An experimental and theoretical insight, *Acta Mater.*, 2009, vol. 57, no. 17, pp. 5174–5185. <https://doi.org/10.1016/j.actamat.2009.07.019>.
26. Rath, M.K., Pradhan, G.K., Pandey, B., Verma, H.C., Roul, B.K., and Anand, S., Synthesis, characterization and dielectric properties of europium-doped barium titanate nanopowders, *Mater. Lett.*, 2008, vol. 62, pp. 2136–2139, <https://doi.org/10.1016/j.matlet.2007.11.033>.
27. Sitko, D., Garbarz-Glos, B., Piekarczyk, W., Smiga, W., and Antonova, M., The effects of the additive of Eu ions on elastic and electric properties of  $\text{BaTiO}_3$  ceramics. *Int. Ferroel.*, 2016, vol. 173, no. 1, pp. 31–37. <http://dx.doi.org/10.1080/10584587.2016.1183413>.
28. Geetha, P., Sarita, P., and Krishna Rao, D., Synthesis, structure, properties and applications of barium titanate nanoparticles. *Int. J. Adv. Tech. Eng. Sci.*, 2016, vol. 4, spec. no. 01, pp. 178–187.
29. Shen Zhigang, Zhang Weiwei, Chen Jianfeng, and Jimmy Yun Low, Temperature one step synthesis of barium titanate: particle formation mechanism and large-scale synthesis, *Chin. J. Chem. Eng.*, 2006, vol. 14, no. 5, pp. 642–648. [https://doi.org/10.1016/S1004-9541\(06\)60128-6](https://doi.org/10.1016/S1004-9541(06)60128-6).
30. Liqiu Wang, Liang Liu, Dongfeng Xue, Hongmin Kang, and Changhou Liu, Wet routes of high purity  $\text{BaTiO}_3$  nanopowders, *J. Alloys Compd.*, 2007, vol. 440 pp. 78–83. <https://doi.org/10.1016/j.jallcom.2006.09.023>.
31. Baorang Li, Xiaohui Wang, and Longtu Li, Synthesis and sintering behavior of  $\text{BaTiO}_3$  prepared by different chemical methods, *Mater. Chem. Phys.* 2002, vol. 78, pp. 292–298. [https://doi.org/10.1016/S0254-0584\(02\)00351-6](https://doi.org/10.1016/S0254-0584(02)00351-6).
32. V. Raghavendra Reddy, Sanjay Kumar Upadhyay, Ajay Gupta, Anand M. Awasthi, and Shamima Hussain, Enhanced dielectric and ferroelectric properties of  $\text{BaTiO}_3$  ceramics prepared by microwave assisted radiant hybrid sintering, *Ceram. Int.*, 2014, vol. 40, no. 6, pp. 8333–8339. <https://doi.org/10.1016/j.ceramint.2014.01.039>.

Translated by N. Korovin